Vietnam Journal of Mechanics, Vol. 44, No. 4 (2022), pp. 418 – 430
DOI: https://doi.org/10.15625/0866-7136/17932

A NEW ANALYTICAL APPROACH OF NONLINEAR THERMAL BUCKLING OF FG-GPLRC CIRCULAR PLATES AND SHALLOW SPHERICAL CAPS USING THE FSDT AND GALERKIN METHOD

Bui Tien Tu[1,2,*], **Le Ngoc Ly**[1], **Nguyen Thi Phuong**[3]
[1]*Faculty of Fundamental Science for Engineering, University of Transport Technology, Hanoi, Vietnam*
[2]*Institute of Transport Technology, University of Transport Technology, Hanoi, Vietnam*
[3]*Faculty of Civil Engineering, University of Transport Technology, Hanoi, Vietnam*
[*]E-mail: tubt@utt.edu.vn

Received: 05 December 2022 / Published online: 30 December 2022

Abstract. A new analytical approach for nonlinear thermal buckling of Functionally Graded Graphene Platelet Reinforced Composite (FG-GPLRC) circular plates and shallow spherical caps using the first-order shear deformation theory (FSDT) is presented in this paper. The circular plates and shallow spherical caps are assumed to be subjected to uniformly distributed thermal loads. By applying the Galerkin method, the relations between thermal load-deflection are achieved to determine the postbuckling behavior and critical buckling loads of the considered structures. Special effects on the nonlinear thermal behavior of circular plates and shallow spherical caps with five different material distribution laws, different Graphene platelet (GPL) mass fractions, and geometrical dimensions are explored and discussed in numerical examples.

Keywords: nonlinear stability, first-order shear deformation theory, FG-GPLRC, thermal load, Galerkin method.

1. INTRODUCTION

The important portions in many engineering structures are constituted by shallow spherical caps, for example, the aircraft, missile, and aerospace components. As a result, the problems relating to mechanic behaviors in the design of this structure have attracted the attention of many researchers.

Functionally graded material (FGM) was proposed to be made from ceramic and metal. Creating from these advantageous properties of two constituent materials, FGM has been used widely in many engineering structures in high-temperature environments such as civil engineering, mechanical engineering, aerospace, nuclear plants, ... Najafizadeh and Hedayati [1] presented the analytical solutions for the thermo-elastic stability of FGM circular plates using the refined theory and adjacent equilibrium criterion. By using the isogeometric finite element formulation, the thermal buckling analysis of FGM circular plates was investigated by Loc et al. [2]. Applying the assumption of the shallowness of the caps, the complex spherical coordinate system was approximated to the polar coordinate system, and the nonlinear buckling and vibration of axisymmetric and un-axisymmetric functionally graded thin shallow spherical caps under uniform external pressure including temperature effects were analyzed by Bich et al. [3, 4]. The thermo-mechanical behavior of the FGM spherical caps was analyzed based on the classical shell theory (CST) and first shear deformation theory (FSDT), using different methods for nonlinear static buckling problem [5], and nonlinear vibration [6,7].

Functionally Graded Graphene Platelet Reinforced Composite (FG-GPLRC) is an advanced composite material, which is created by reinforcing the graphene platelet (GPL) into the isotropic matrix, becoming popular in engineering design. Many authors focused on the static and dynamic behavior of many types of FG-GPLRC structures. However, a few reports of FG-GPLRC shallow spherical caps are obtained in the open literature. Huo et al. [8] studied the bending problem of circular/annular sector FG-GPLRC plates by applying a 3D-poroflexibility theory. The three-dimensional elasticity solutions for the free vibration and bending of the FG-GPLRC spherical caps were analyzed by Liu et al. [9].

This paper presents a new analytical approach to investigate the nonlinear thermal buckling of FG-GPLRC circular plates and shallow spherical caps with the clamped boundary condition at the edge by using the FSDT and Galerkin method. The effects of geometrical and material properties on the buckling behavior of circular plates and spherical caps with five different material distribution laws of GPL are investigated and discussed in numerical examples.

2. GEOMETRICAL AND MATERIAL PROPERTIES

Consider the FG-GPLRC shallow spherical caps/circular plates with radius of curvature R, base radius a, thickness h, and the coordinate system (r, θ, z) as shown in Fig. 1. Five distribution laws of GPL are considered to be UD-GPLRC, X-GPLRC, O-GPLRC, A-GPLRC, and V-GPLRC. The shallow spherical caps/circular plates are subjected to uniformly distributed thermal loads with the clamped boundary condition at the edge.

The Young's modulus of the spherical caps/circular plates is determined based on the extended Halpin–Tsai model as follows [10]

$$E\left(z\right) = \frac{3}{8}\frac{1+\zeta_1\delta_1 V_{GPL}\left(z\right)}{1-\delta_1 V_{GPL}\left(z\right)}E_m + \frac{5}{8}\frac{1+\zeta_2\delta_2 V_{GPL}\left(z\right)}{1-\delta_2 V_{GPL}\left(z\right)}E_{m}, \tag{1}$$

where

$$\delta_1 = \frac{\left(E_{GPL}/E_m\right)-1}{\left(E_{GPL}/E_m\right)+\zeta_1},\ \delta_2 = \frac{\left(E_{GPL}/E_m\right)-1}{\left(E_{GPL}/E_m\right)+\zeta_2},\ \zeta_1 = 2\left(\frac{a_{GPL}}{t_{GPL}}\right),\ \zeta_2 = 2\left(\frac{b_{GPL}}{t_{GPL}}\right), \tag{2}$$

with E_m and E_{GPL} are respectively the elastic moduli of the matrix and GPL, a_{GPL}, b_{GPL} and t_{GPL} are the length, width and thickness of the GPL, respectively, and V_{GPL} is the

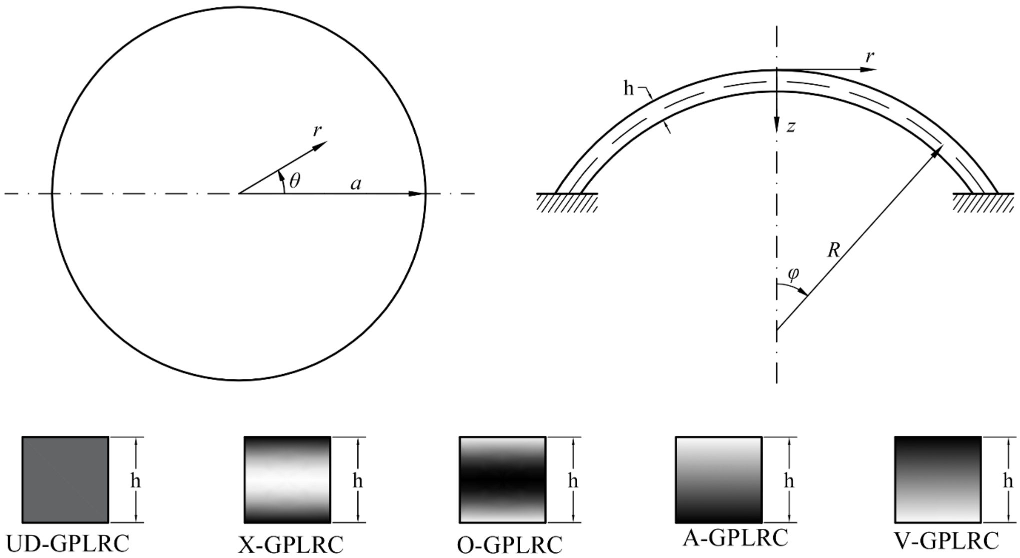

Fig. 1. Configuration of shallow spherical caps/circular plates, and five distribution laws of GPL

volume fraction of the GPL $(V_m + V_{GPL} = 1)$ defined as

$$V_{GPL}\left(z\right) = \frac{W_{GPL}}{W_{GPL} + \left(\rho_{GPL}/\rho_m\right)\left(1 - W_{GPL}\right)}, \tag{3}$$

where ρ_m and ρ_{GPL} are the densities of the matrix and the GPL, respectively, W_{GPL} is the mass fraction of GPL which depends on five distribution laws of GPL of spherical caps/circular plates with the following functions

$$W_{GPL}\left(z\right) = \begin{cases} W^*_{GPL} & \text{for} \quad \dfrac{-h}{2} \le z \le \dfrac{h}{2} \quad \text{UD - GPLRC}, \\ 4\dfrac{|z|}{h}W^*_{GPL} & \text{for} \quad \dfrac{-h}{2} \le z \le \dfrac{h}{2} \quad \text{X - GPLRC}, \\ 2\left(1 - \dfrac{2\,|z|}{h}\right)W^*_{GPL} & \text{for} \quad \dfrac{-h}{2} \le z \le \dfrac{h}{2} \quad \text{O - GPLRC}, \\ \left(1 - \dfrac{2z}{h}\right)W^*_{GPL} & \text{for} \quad \dfrac{-h}{2} \le z \le \dfrac{h}{2} \quad \text{V - GPLRC}, \\ \left(1 + \dfrac{2z}{h}\right)W^*_{GPL} & \text{for} \quad \dfrac{-h}{2} \le z \le \dfrac{h}{2} \quad \text{A - GPLRC}, \end{cases} \tag{4}$$

where W^*_{GPL} is denote of total mass fraction of GPL.

According to the rule of mixture, the Poisson's ratio and thermal expansion coefficient of FG-GPLRC shallow spherical caps/circular plates are determined as

$$\begin{aligned} \nu\left(z\right) &= \nu_m\left(1 - V_{GPL}\right) + \nu_{GPL}V_{GPL}, \\ \alpha\left(z\right) &= \alpha_m\left(1 - V_{GPL}\right) + \alpha_{GPL}V_{GPL}. \end{aligned} \tag{5}$$

3. ESTABLISHMENT PROCESS OF GOVERNING EQUATIONS

Due to the assumption that the shallow spherical caps/circular plates are axisymmetrically deformed, based on the FSDT, displacement components at any point at a distance z from the mid-surface are determined as

$$\bar{u}\left(r,z\right) = u\left(r\right) + z\psi\left(r\right),\ \bar{v}\left(r,z\right) = 0,\ \bar{w}\left(r,z\right) = w\left(r\right) + w^{*}\left(r\right), \tag{6}$$

where $w^{*}\left(r\right)$ is the initial imperfect deflection of spherical caps.

Hooke's law is applied to the FG-GPLRC shallow spherical caps/circular plates, taking into account the thermal strains, presented as

$$\left\{\begin{array}{c}\sigma_r\\ \sigma_\theta\end{array}\right\} = \left[\begin{array}{cc}Q_{11} & Q_{12}\\ Q_{12} & Q_{22}\end{array}\right]\left\{\begin{array}{c}\varepsilon_r\\ \varepsilon_\theta\end{array}\right\} - \left[\begin{array}{cc}Q_{11} & Q_{12}\\ Q_{12} & Q_{22}\end{array}\right]\left\{\begin{array}{c}\alpha\Delta T\\ \alpha\Delta T\end{array}\right\},\quad \sigma_{rz} = Q_{44}\varepsilon_{rz}, \tag{7}$$

where ΔT is the uniformly distributed thermal load, and the reduced stiffnesses can be determined as

$$Q_{11} = Q_{22} = \frac{E\left(z\right)}{1-\left[\nu\left(z\right)\right]^2},\quad Q_{12} = \frac{E\left(z\right)\nu\left(z\right)}{1-\left[\nu\left(z\right)\right]^2},\quad Q_{44} = \frac{E\left(z\right)}{2\left[1+\nu\left(z\right)\right]}. \tag{8}$$

The strain components of the shallow spherical caps are defined as

$$\left\{\begin{array}{c}\varepsilon_r\\ \varepsilon_\theta\\ \varepsilon_{rz}\end{array}\right\} = \left\{\begin{array}{c}\varepsilon_r^0 + z\chi_r\\ \varepsilon_\theta^0 + z\chi_\theta\\ \psi + w_{,r}\end{array}\right\}, \tag{9}$$

where $\varepsilon_r^0, \varepsilon_\theta^0$ are the strains at the mid-surface, χ_r, χ_θ are curvature constituents, expressed as

$$\left\{\begin{array}{c}\varepsilon_r^0\\ \varepsilon_\theta^0\end{array}\right\} = \left\{\begin{array}{c}u_{,r} - \dfrac{w}{R} + \dfrac{1}{2}w_{,r}^2 + w_{,r}w_{,r}^{*}\\ \dfrac{u}{r} - \dfrac{w}{R}\end{array}\right\},\qquad \left\{\begin{array}{c}\chi_r\\ \chi_\theta\end{array}\right\} = \left\{\begin{array}{c}\psi_{,r}\\ \dfrac{\psi}{r}\end{array}\right\}. \tag{10}$$

The forces and moments are determined by

$$\left(N_r, M_r\right) = \int\limits_{-h/2}^{h/2}(1,z)\sigma_r \mathrm{d}z,\ \left(N_\theta, M_\theta\right) = \int\limits_{-h/2}^{h/2}(1,z)\sigma_\theta \mathrm{d}z,\ Q_r = \int\limits_{-h/2}^{h/2}\sigma_{rz}\mathrm{d}z. \tag{11}$$

Substituting Eq. (9) into Eq. (7), and then substituting the resultant equations into Eq. (11), the force and moment expressions are obtained

$$\left\{\begin{array}{c}N_r\\ N_\theta\\ M_r\\ M_\theta\end{array}\right\} = \left\{\begin{array}{cccc}A_{11} & A_{12} & B_{11} & B_{12}\\ A_{12} & A_{22} & B_{12} & B_{22}\\ B_{11} & B_{12} & D_{11} & D_{12}\\ B_{12} & B_{22} & D_{12} & D_{22}\end{array}\right\}\left\{\begin{array}{c}\varepsilon_r^0\\ \varepsilon_\theta^0\\ \chi_r\\ \chi_\theta\end{array}\right\} - \left\{\begin{array}{c}\Phi_1\\ \Phi_1\\ \Phi_2\\ \Phi_2\end{array}\right\},\qquad Q_r = K_s H_{44}\left(\psi + w_{,r}\right), \tag{12}$$

where

$$H_{44} = \int\limits_{-h/2}^{h/2} Q_{44}\mathrm{d}z,\quad \Phi_1 = \Delta T\Phi_1^{*},\quad \Phi_1^{*} = \int\limits_{-h/2}^{h/2}\left(Q_{11}+Q_{12}\right)\alpha \mathrm{d}z, \tag{13}$$

where $K_s = \dfrac{5}{6}$ is the shear correction factor.

The nonlinear equilibrium equations of shallow spherical caps/circular plates are

$$\begin{aligned} &(rN_r)_{,r} - N_\theta = 0, \qquad (rM_r)_{,r} - M_\theta - rQ_r = 0, \\ &(rQ_r)_{,r} + \frac{r}{R}(N_r + N_\theta) + \left[rN_r \left(w_{,r} + w^*_{,r} \right) \right]_{,r} = 0. \end{aligned} \tag{14}$$

Substituting Eq. (10) into the forces and moments (12), then substituting the result into Eq. (14), the equilibrium equation system is rewritten by

$$\begin{aligned} L_1 \equiv & -\frac{B_{22}\psi}{r} + B_{11}\psi_{,r} - \frac{rA_{11}w_{,r}}{R} + rA_{11}w_{,r}w_{,rr} + rA_{11}w_{,rr}w^*_{,r} + rA_{11}w_{,r}w^*_{,rr} \\ & - \frac{rA_{12}w_{,r}}{R} + A_{11}u_{,r} + \frac{A_{11}w^2_{,r}}{2} - \frac{A_{12}w^2_{,r}}{2} - \frac{A_{11}w}{R} - \frac{A_{22}u}{r} + \frac{A_{22}w}{R} \\ & + rB_{11}\psi_{,rr} - A_{12}w_{,r}w^*_{,r} + A_{11}w_{,r}w^*_{,r} + rA_{11}u_{,rr} = 0, \end{aligned} \tag{15}$$

$$\begin{aligned} L_2 \equiv & B_{11}u_{,r} + \frac{B_{11}w^2_{,r}}{2} - \frac{B_{12}w^2_{,r}}{2} - \frac{rB_{11}w_{,r}}{R} + rB_{11}w_{,r}w_{,rr} + rB_{11}w_{,rr}w^*_{,r} \\ & + rB_{11}w_{,r}w^*_{,rr} - \frac{rB_{12}w_{,r}}{R} - K_sH_{44}r\psi - K_sH_{44}rw_{,r} + rB_{11}u_{,rr} + B_{11}w_{,r}w^*_{,r} \\ & - \frac{B_{11}w}{R} - \frac{B_{22}u}{r} + \frac{B_{22}w}{R} + rD_{11}\psi_{,rr} - B_{12}w_{,r}w^*_{,r} - \frac{D_{22}\psi}{r} + D_{11}\psi_{,r} = 0, \end{aligned} \tag{16}$$

$$\begin{aligned} L_3 \equiv & \frac{A_{11}w^3_{,r}}{2} - w_{,r}\Phi^*_1\Delta T - w^*_{,r}\Phi^*_1\Delta T + w^*_{,r}A_{11}u_{,r} + \frac{3A_{11}w^2_{,r}w^*_{,r}}{2} + w^*_{,r}B_{11}\psi_{,r} \\ & - rw^*_{,rr}\Phi^*_1\Delta T + w_{,r}A_{11}u_{,r} - \frac{2r\Phi^*_1\Delta T}{R} + K_sH_{44}w_{,r} + A_{11}w_{,r}\left(w^*_{,r}\right)^2 - rw_{,rr}\Phi^*_1\Delta T \\ & + w_{,r}B_{11}\psi_{,r} + K_sH_{44}\psi + 3rw_{,r}A_{11}w_{,rr}w^*_{,r} - \frac{rw_{,rr}A_{11}w}{R} - \frac{rw_{,rr}A_{12}w}{R} \\ & + 2rw^*_{,r}A_{11}w_{,r}w^*_{,rr} - \frac{rw^*_{,rr}A_{11}w}{R} - \frac{rw^*_{,rr}A_{12}w}{R} + \frac{rB_{11}\psi_{,r}}{R} + \frac{B_{12}\psi}{R} + \frac{rA_{12}u_{,r}}{R} - \frac{rA_{12}w^2_{,r}}{2R} \\ & + \frac{A_{22}u}{R} - \frac{rA_{22}w}{R^2} + \frac{rB_{12}\psi_{,r}}{R} + \frac{B_{22}\psi}{R} + rw_{,r}A_{11}u_{,rr} + \frac{3rw^2_{,r}A_{11}w_{,rr}}{2} + \frac{3rw^2_{,r}A_{11}w^*_{,rr}}{2} \\ & + w_{,r}A_{12}u_{,r} + rw_{,r}B_{11}\psi_{,rr} + w_{,r}B_{12}\psi_{,r} - \frac{w_{,r}A_{11}w}{R} - \frac{w_{,r}A_{12}w}{R} + rw_{,rr}A_{11}u_{,r} + w_{,rr}A_{12}u \\ & + rw_{,rr}B_{11}\psi_{,r} + w_{,rr}B_{12}\psi + rw^*_{,r}A_{11}u_{,rr} + r\left(w^*_{,r}\right)^2 A_{11}w_{,rr} + w^*_{,r}A_{12}u_{,r} + rw^*_{,r}B_{11}\psi_{,rr} \\ & + w^*_{,r}B_{12}\psi_{,r} - \frac{w^*_{,r}A_{11}w}{R} - \frac{w^*_{,r}A_{12}w}{R} + rw^*_{,rr}A_{11}u_{,r} + w^*_{,rr}A_{12}u + rw^*_{,rr}B_{11}\psi_{,r} + w^*_{,rr}B_{12}\psi \\ & + K_sH_{44}r\psi_{,r} + K_sH_{44}rw_{,rr} + \frac{rA_{11}u_{,r}}{R} - \frac{rA_{11}w}{R^2} - \frac{rA_{11}w^2_{,r}}{2R} + \frac{A_{12}u}{R} - \frac{2rA_{12}w}{R^2} = 0. \end{aligned} \tag{17}$$

4. BOUNDARY CONDITION AND SOLVING PROBLEM

In this paper, the FG-GPLRC shallow spherical caps/circular plates are assumed to be clamped and immovable at the edge, subjected to uniformly distributed thermal loads. The following approximate solutions for the displacement components and rotation are assumed to be in the forms

$$u = U \sin \frac{\pi r}{a}, \quad \psi = \Psi \sin \frac{\pi r}{a}, \quad w = W \cos^2 \frac{\pi r}{2a}, \quad w^* = W^* \cos^2 \frac{\pi r}{2a}, \tag{18}$$

where U, W, and Ψ are maximal displacement constituents and rotation, W^* is maximal imperfection.

Substituting the solution forms (18) into equilibrium equations (15)–(17) and applying the Galerkin method, leads to

$$X_{11}W^2 + X_{12}W + X_{13}U + X_{14}\Psi = 0, \tag{19}$$

$$X_{21}W^2 + X_{22}W + X_{23}U + X_{24}\Psi = 0, \tag{20}$$

$$X_{31}W^3 + X_{32}W^2 + \left(X_{33}U + X_{34}\Psi + X_{35} + \frac{\pi^2 \Phi_1^* \Delta T}{16} \right) W + X_{36}U + X_{37}\Psi + X_{38}\Phi_1^* \Delta T = 0, \tag{21}$$

The expressions of $U$and Ψ can be solved from Eqs. (19) and (20), and substituting them into Eq. (21), leads to

$$\begin{aligned} &\left(\begin{array}{l} X_{31} - \dfrac{X_{33}\left(X_{11}X_{24} - X_{14}X_{21}\right)}{X_{13}X_{24} - X_{14}X_{23}} \\ + \dfrac{X_{34}\left(X_{11}X_{23} - X_{13}X_{21}\right)}{X_{13}X_{24} - X_{14}X_{23}} \end{array} \right) W^3 + \left(\begin{array}{l} X_{32} - \dfrac{X_{33}\left(X_{12}X_{24} - X_{14}X_{22}\right)}{X_{13}X_{24} - X_{14}X_{23}} \\ + \dfrac{X_{34}\left(X_{12}X_{23} - X_{13}X_{22}\right)}{X_{13}X_{24} - X_{14}X_{23}} \\ - \dfrac{X_{36}\left(X_{11}X_{24} - X_{14}X_{21}\right)}{X_{13}X_{24} - X_{14}X_{23}} \\ + \dfrac{X_{37}\left(X_{11}X_{23} - X_{13}X_{21}\right)}{X_{13}X_{24} - X_{14}X_{23}} \end{array} \right) W^2 \\ &+ \left(\begin{array}{l} X_{35} - \dfrac{X_{36}\left(X_{12}X_{24} - X_{14}X_{22}\right)}{X_{13}X_{24} - X_{14}X_{23}} \\ + \dfrac{X_{37}\left(X_{12}X_{23} - X_{13}X_{22}\right)}{X_{13}X_{24} - X_{14}X_{23}} \end{array} \right) W = -\left(\frac{\pi^2 \Phi_1^*}{16} W + X_{38}\Phi_1^* \right) \Delta T. \end{aligned} \tag{22}$$

In the case of perfect circular plates $(W^* = 0, R \to \infty)$, the thermal critical buckling loads ΔT_{cr} (K) can be determined by applying $W \to 0$ in Eq. (22), as

$$\Delta T_{cr} = -\frac{16}{\pi^2 \Phi_1^*} \left[X_{35} - \frac{X_{36}\left(X_{12}X_{24} - X_{14}X_{22}\right)}{X_{13}X_{24} - X_{14}X_{23}} + \frac{X_{37}\left(X_{12}X_{23} - X_{13}X_{22}\right)}{X_{13}X_{24} - X_{14}X_{23}} \right]. \tag{23}$$

5. NUMERICAL RESULTS AND DISCUSSIONS

5.1. Validation

Consider the clamped FGM circular plates subjected to uniformly distributed thermal loads. Table 1 compared the thermal critical buckling loads of present results with those of the adjacent equilibrium criterion solutions [1] and the isogeometric finite element solutions [2] using FSDT and HSDT, respectively. Clearly, good agreements can be observed in these comparisons.

Table 1. Comparison of thermal critical buckling loads (K) of FGM circular plates with previous results

	h/a				
	0.05	0.04	0.03	0.02	0.01
FSDT [1]	146.8150	94.0810	53.0290	23.6030	5.9060
HSDT [2]	144.9953	93.4005	52.8191	23.5719	5.9093
Present	147.0435	94.4065	53.2351	23.7019	5.9318

5.2. Numerical examples

In this sub-section, material properties and efficiency parameters of GPLs and copper matrix are chosen as the report of Wang et al. [10]. The effects of the mass fraction of GPL, geometric ratio a/h and distribution laws on the thermal critical buckling loads of circular plates are presented in Table 2. As can be seen, when the mass fraction of the GPL increases, the thermal critical buckling load of plates increases for the four distribution laws UD-GPLRC, X-GPLRC, V-GPLRC, and A-GPLRC, in which the largest critical buckling loads are obtained for X-GPLRC plates. Especially, an abnormal tendency can be observed for O-GPLRC plates. In addition, the thermal critical buckling load increases strongly as the geometric ratio a/h decreases in all investigated cases.

Effects of GPL distribution law on the thermal load-deflection postbuckling curves of FG-GPLRC circular plates and shallow spherical caps are presented in Figs. 2 and 3. The results show that with the same mass fraction of GPL and geometrical parameters, the thermal load-deflection postbuckling curves of X-GPLRC circular plates and shallow spherical caps are the highest, and those of the O-GPLRC are the lowest. The difference between the five thermal load-deflection postbuckling curves in the circular plates is more clearly observable than that of the shallow spherical caps. The bifurcation points can be observed for FG-GPLRC circular plates, oppositely, those can not be obtained for FG-GPLRC spherical caps.

Table 2. The effects of mass fraction of GPL, geometric ratio a/h and GPL distribution laws on thermal critical buckling loads ΔT_{cr} (K) of circular plates

a/h	W^*_{GPL} (%)	$h = 0.01$ m, $R = \infty$				
		UD-GPLRC	X-GPLRC	O-GPLRC	V-GPLRC	A-GPLRC
40	0	33.61831326	33.61831326	33.61831326	33.61831326	33.61831326
	1	35.91610556	41.76246442	30.31616008	34.65249896	34.65249896
	5	44.51537154	56.71370989	33.11716246	39.42070236	39.42070236
	9	52.25587898	65.80692333	38.52783669	45.06256432	45.06256432
30	0	59.63674508	59.63674508	59.63674508	59.63674508	59.63674508
	1	63.71532393	74.06237924	53.79942516	61.47908230	61.47908230
	5	78.97876715	100.5714835	58.78860685	69.95894562	69.95894562
	9	92.71772993	116.7070385	68.39685692	79.97840643	79.97840643
20	0	133.3591719	133.3591719	133.3591719	133.3591719	133.3591719
	1	142.4953013	165.4813810	120.4360026	137.5283674	137.5283674
	5	176.6838855	224.6757533	131.7226049	156.6268534	156.6268534
	9	207.4561664	260.7879465	153.2719414	179.1029284	179.1029284

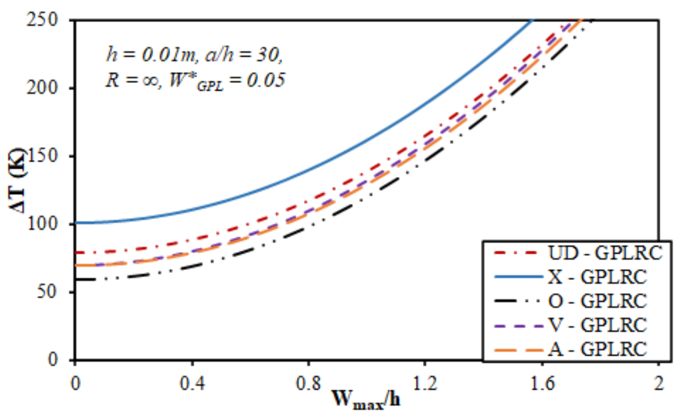

Fig. 2. Effect of GPL distribution law on the thermal load-deflection postbuckling curves of FG-GPLRC circular plates

Figs. 4 and 5 show the large effects of the mass fraction of GPL on the thermal load-deflection postbuckling curves of UD-GPLRC circular plates and X-GPLRC shallow spherical caps, respectively. Obviously, the deflections of circular plates and shallow spherical caps decrease rapidly as the mass fraction of GPL increases for both cases.

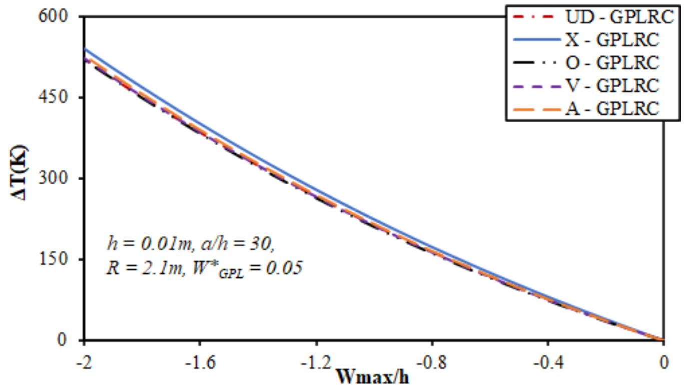

Fig. 3. Effect of GPL distribution law on the thermal load-deflection postbuckling curves of FG-GPLRC shallow spherical caps

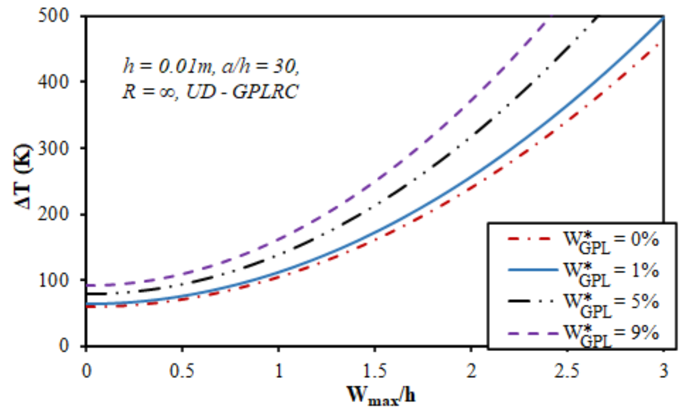

Fig. 4. Effect of mass fraction of GPL on the thermal load-deflection postbuckling curves of UD-GPLRC circular plates

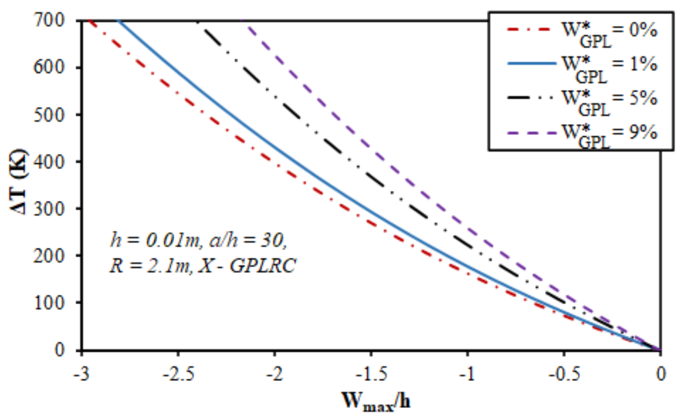

Fig. 5. Effect of mass fraction of GPL on the thermal load-deflection postbuckling curves of X-GPLRC shallow spherical caps

Figs. 6–9 present the thermal load-deflection postbuckling curves of circular plates and shallow spherical caps with different geometrical ratios a/R and a/h, applied to three distribution laws of GPL: X-GPLRC, O-GPLRC, and V-GPLRC. Clearly, the thermal load-deflection postbuckling curves of circular plates and shallow spherical caps are gradually lower as the geometrical ratio a/R decreases for all three GPL distribution laws. Conversely, those are gradually upper when the geometrical ratio a/h increases.

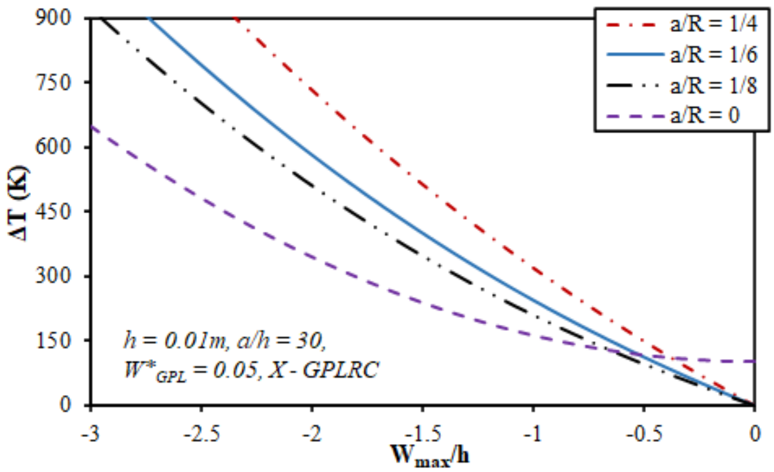

Fig. 6. Effect of a/R ratio on the thermal load-deflection postbuckling curves of X-GPLRC shallow spherical caps

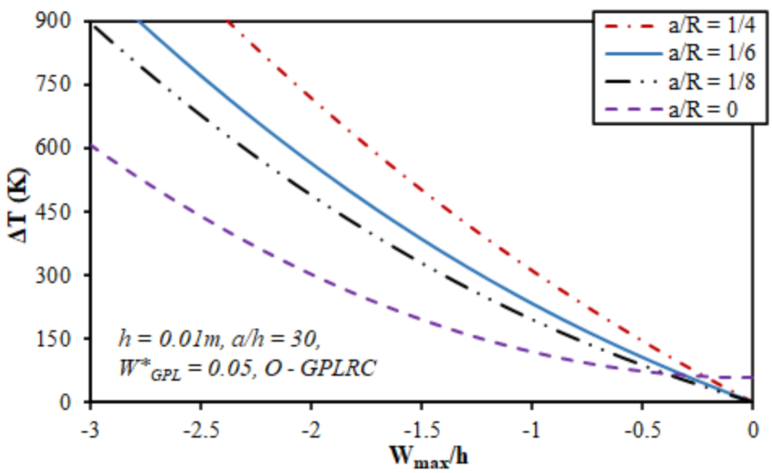

Fig. 7. Effect of a/R ratio on the thermal load-deflection postbuckling curves of O-GPLRC shallow spherical caps

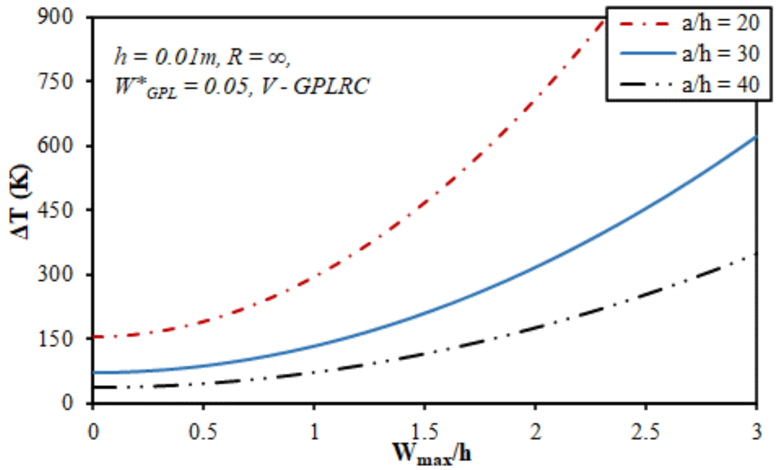

Fig. 8. Effect of a/h ratio on the thermal load-deflection postbuckling curves of V-GPLRC circular plates

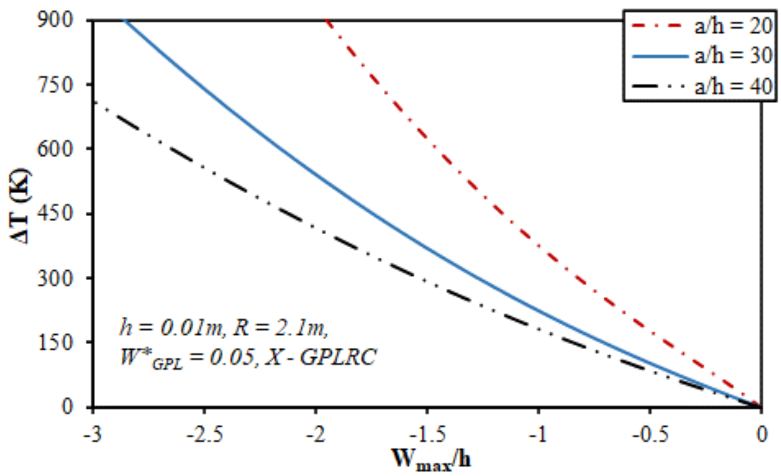

Fig. 9. Effect of a/h ratio on the thermal load-deflection postbuckling curves of X-GPLRC shallow spherical caps

6. CONCLUSIONS

This paper presents an analytical approach of nonlinear thermal buckling of axisymmetrical FG-GPLRC circular plates and shallow spherical caps. The governing equations are derived by using the FSDT with von Karman geometrical nonlinearity, and the equilibrium equations are solved by the Galerkin method. Numerical results show that:

- When the mass fraction of the GPL increases, the thermal critical buckling load of plates increases for the four distribution laws UD-GPLRC, X-GPLRC, V-GPLRC, and

A-GPLRC, in which the largest critical buckling loads are obtained for X-GPLRC plates. Especially, an abnormal tendency can be observed for O-GPLRC plates;

- The load-carrying capacities of the shallow spherical caps and circular plates both increase markedly with the increase in the mass fraction of the GPL;

- The large effects of geometrical ratios on the critical buckling loads and postbuckling curves of circular plates and spherical caps can be also obtained from investigated examples.

DECLARATION OF COMPETING INTEREST

The authors declare that they have no known competing financial interests or personal relationships that could have appeared to influence the work reported in this paper.

FUNDING

This research received no specific grant from any funding agency in the public, commercial, or not-for-profit sectors.

REFERENCES

[1] M. M. Najafizadeh and B. Hedayati. Refined theory for thermoelastic stability of functionally graded circular plates. *Journal of Thermal Stresses*, **27**, (2004), pp. 857–880. https://doi.org/10.1080/01495730490486532.

[2] L. V. Tran, C. H. Thai, and H. Nguyen-Xuan. An isogeometric finite element formulation for thermal buckling analysis of functionally graded plates. *Finite Elements in Analysis and Design*, **73**, (2013), pp. 65–76. https://doi.org/10.1016/j.finel.2013.05.003.

[3] D. H. Bich, D. V. Dung, and V. H. Nam. Nonlinear axisymmetric dynamic buckling and vibration of functionally graded shallow spherical shells under external pressure including temperature effects resting on elastic foundation. In *Vietnam National Conference on Mechanics of Deformable Solids*, Ho Chi Minh City, (2013), pp. 101–110.

[4] D. H. Bich, D. V. Dung, and V. H. Nam. Nonlinear axisymmetric dynamic analysis of shallow spherical shells with functionally graded coatings under external pressure including temperature effects and resting on elastic foundation. In *Vietnam National Conference on Mechanic Engineering*, Hanoi, (2014), pp. 25–30.

[5] R. Shahsiah, M. R. Eslami, and R. Naj. Thermal instability of functionally graded shallow spherical shell. *Journal of Thermal Stresses*, **29**, (2006), pp. 771–790. https://doi.org/10.1080/01495730600705406.

[6] N. T. Phuong, V. H. Nam, and D. T. Dong. Nonlinear vibration of functionally graded sandwich shallow spherical caps resting on elastic foundations by using first-order shear deformation theory in thermal environment. *Journal of Sandwich Structures & Materials*, **22**, (2018), pp. 1157–1183. https://doi.org/10.1177/1099636218782645.

[7] T. Q. Minh, D. T. Dong, V. M. Duc, N. V. Tien, N. T. Phuong, and V. H. Nam. Nonlinear axisymmetric vibration of sandwich FGM shallow spherical caps with lightweight porous core. In *Lecture Notes in Civil Engineering*, pp. 381–389. Springer Singapore, (2021). https://doi.org/10.1007/978-981-16-7160-9_38.

[8] J. Huo, G. Zhang, A. Ghabussi, and M. Habibi. Bending analysis of FG-GPLRC axisymmetric circular/annular sector plates by considering elastic foundation and horizontal friction force using 3D-poroelasticity theory. *Composite Structures*, **276**, (2021). https://doi.org/10.1016/j.compstruct.2021.114438.

[9] D. Liu, Y. Zhou, and J. Zhu. On the free vibration and bending analysis of functionally graded nanocomposite spherical shells reinforced with graphene nanoplatelets: Three-dimensional elasticity solutions. *Engineering Structures*, **226**, (2021). https://doi.org/10.1016/j.engstruct.2020.111376.

[10] Y. Wang, R. Zeng, and M. Safarpour. Vibration analysis of FG-GPLRC annular plate in a thermal environment. *Mechanics Based Design of Structures and Machines*, **50**, (2020), pp. 352–370. https://doi.org/10.1080/15397734.2020.1719508.